Superlattices and Microstructures 138 (2020) 106377

Contents lists available at ScienceDirect

Superlattices and Microstructures

journal homepage: www.elsevier.com/locate/superlattices

Enhancement of the efficiency of ultra-thin CIGS/Si structure for solar cell applications

M. Boubakeur [a], A. Aissat [a,c,*], M. Ben Arbia [b], H. Maaref [b], J.P. Vilcot [c]

[a] Faculty of Technology University of Blida.1, 09000, Blida, Algeria
[b] Laboratoire de Micro-Optoelectronique et Nanostructures, Departement de Physique, Faculte des Sciences de Monastir, 5019, Avenue de l'environnement, Universite de Monastir, Tunisia
[c] Institut d'Electronique, de Microelectronique et de Nanotechnologie (IEMN), UMR CNRS 8520, Universite' des Sciences et Technologies de Lille 1, Avenue Poincare', BP 60069, 59652, Villeneuve d'Ascq, France

ARTICLE INFO

Keywords:
Materials
Ultra-thin CIGS
Thickness
Conversion efficiency
Solar cell

ABSTRACT

This paper describes a numerical study of ultrathin CIGS solar cell using the one-dimensional simulation program. The various properties of the absorber layer such as the band gap energy, the absorption coefficient, and the reflection coefficient are investigated. In addition, the impact of adding silicon to reduce the thickness of CIGS is also examined. We have carried out a theoretical study to show the influence of the thickness and the gallium concentration of the CIGS absorber layer on the performance of the Mo/Si/CIGS/ZnS/ZnO structure. It has been demonstrated that increasing x_{Ga} and d_{CIGS} affect the conversion efficiency, FF, $V_{oc,}$ and J_{sc}. Finally, we have achieved a conversion efficiency $\eta = 21.08\%$ with an optimal value of gallium content equal to 20%when the thickness of the absorber layer has been reduced to 0.75 μm. This study allowed us to improve the performance of thin film solar cell.

1. Introduction

Silicon cell technology has emerged since the past decades for photovoltaic application thanks to the high absorption coefficient and the important diffusion length. More interestingly, several researches have been devoted to study III-V and II-VI materials in order to exploit the entire solar cells, thereby improving the photovoltaic yield. These materials have been stacked for tandem and multi-junction solar cells reaching 30% [1–4] and 50% [5,6] of efficiency, respectively. However, these devices require high production cost and more sophisticated elaboration techniques. For this reason, we have assigned to study thin films based on such materials: CdTe, Cu_2ZnSnS_4, $CuInGaSe_2$ … etc., reported in the literature [7–9].

In the following, we have a focus on $CuInGaSe_2$ quaternary which is considered the most advanced and efficient alternative in thin-film technology with important conversion yield ranged from 21 to 22.6% [10,11] using CdS and ZnS as buffer layers for 2–3 μm of CIGS thickness. This chalcopyrite is characterized by an absorption coefficient around 10^4-10^5 [12] and altered band gap energy which can be monitored by Ga concentration. The best energy value is almost 1.14 eV, according to $x_{Ga} = 0.30$ [13] that represents the optimal concentration obtained for low defect density as reported in Ref. [14].

In order to improve solar cell performance, we should obtain a compromise between manufacturing cost and high-value efficiency. In this context, it is necessary to reduce the thickness of CIGS absorber [15]. However, it has been stipulated in Ref. [16] that growing

* Corresponding author. Faculty of Technology University of Blida.1, 09000, Blida, Algeria.
E-mail address: sakre23@yahoo.fr (A. Aissat).

https://doi.org/10.1016/j.spmi.2019.106377
Received 31 August 2019; Received in revised form 10 December 2019; Accepted 16 December 2019
Available online 19 December 2019

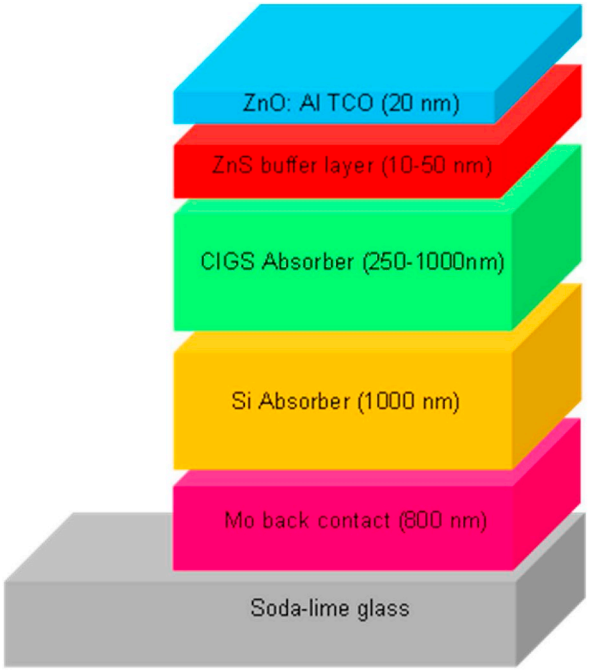

Fig. 1. Schematic view of ZnO/ZnS/CIGS/Si/Mo structure.

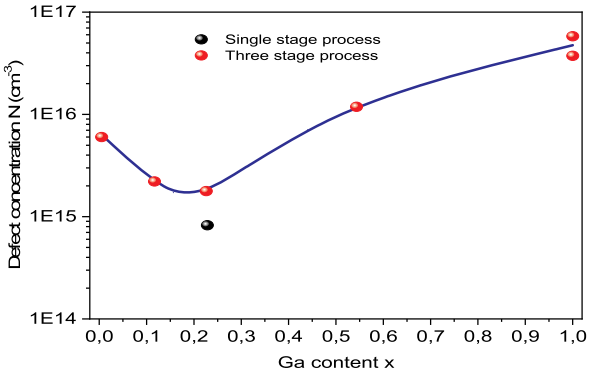

Fig. 2. Bulk defect concentration N as function of gallium concentration [14].

ultra-thin CIGS layer on Mo, with thickness less than 0.5 μm can degrade the photovoltaic efficiency significantly by dint of recombination losses and poor reflectivity at CIGS/Mo interface.

On the theoretical side, M. Gloeckler et al. have mentioned that thinning down CIGS layer from 3 to 0.3 μm entails above 17% of conversion efficiency for passivated CIGS layer [17]. B. Vermang et al. have experimentally designed the following structure: ZnO: Al/i-ZnO/CdS/CIGS/Mo deposited on lime glass soda and reached above 9% of conversion efficiency. An Al2O3-passivation of 0.385 μm-CIGS absorber enhances the efficiency to 17% [16].

Recently, L. M. Mansfield et al. have developed an ultra-thin CIGS-based solar device by the mean of three-stage technique with performing MgF2-antireflective coating. The non-passivated structure has achieved efficiency around 15.2% [18].

A new CIGS-based structure (ZnO/CdS/CIGS/Si) has been proposed by H. Heriche et al. [19]. They have demonstrated that the inserted Si layer as the second absorber, boosts the solar cell efficiency from 16.39% to 21.3%. Additionally, J. Goffard et al. have designed nanostructured back mirrors in order to improve the light trapping process in ultra-thin CIGS absorber (<0.5 μm) [20] reaching an efficiency of 20%.

Here, we have suggested introducing a 1 μm-silicon layer in the simulated structure ZnO/ZnS/CIGS/Mo to boost the number of absorbed photons, thereby ensure high efficiency.

Fig. 1 presents the solar cell structure that includes a thin film made from zinc oxide ZnO:Al as the window layer, zinc sulfide ZnS as buffer layer (replacing CdS with ZnS to avoid the toxicity of cadmium) [21,22], p-type CIGS and p-type Si as absorber layers to guarantee higher absorption of photons. Molybdenum is considered as back contact deposited on glass substrate.

In this paper, we have studied the influence of the gallium content and the CIGS thickness on photovoltaic parameters. Moreover, we have determined the optimal value of Ga concentration, taking into consideration the density of the defects according to the work of G. Hanna et al. [14] (Fig. 2). Based on this investigation, we have set the range of gallium concentration $x_{Ga} = 0.10, 0.20, 0.30, 0.40$, where the defects are minimal.

2. Materials and methods

This section identifies physical models, empirical equations, and material parameters applied in this simulation:

SCAPS solves fundamental semiconductor equations in a single dimension. This includes the continuity equations for holes and electrons and the Poison's equation for electrostatic potential ψ [23].

- The continuity equations for electrons and holes are, correspondingly:

$$\frac{1}{q}.\frac{\partial J_n}{\partial x} + G - R_n(n,p) = \frac{\partial n}{\partial t} \tag{1}$$

$$-\frac{1}{q}.\frac{\partial J_p}{\partial x} + G - R_p(n,p) = \frac{\partial p}{\partial t} \tag{2}$$

Where G is the generation rate R is the recombination rate J_n and J_p are respectively electron and hole current density.

- Poisson's equation used is:

$$\frac{\partial}{\partial x}\left(\varepsilon(x)\frac{\partial \Psi}{\partial x}\right) = -\frac{q}{\varepsilon_o}.\left[-n + p + N_D^+ - N_A^- + \frac{1}{q}\rho_{def}(n,p)\right] \tag{3}$$

With ε is the dielectric constant, ψ is the electrostatic potential, p and n Are the free carrier concentrations for hole and electron, N_p^- and N_D^+ are the density of ionized acceptor and donor and ρ_{def} is the space charge density.

- Fermi-Dirac statistic is given by the following equation [24]:

$$f\ (E) = \frac{1}{1 + \exp\left[\frac{E - E_f}{K_B T}\right]} \tag{4}$$

Where E the energy level of a particle is, E_f is the equilibrium Fermi level energy, K_B is the Boltzmann constant and T is the temperature.

- The band gap energy of CIGS as a function of Ga concentration is defined as [25]:

$$E_g^{CIGS} = xE_g^{CIS} + (1 - x)E_g^{CGS} - 0.246.x(1 - x) \tag{5}$$

where E_{gCIS} and E_{gCGS} are respectively the bandgap energies of $CuInSe_2$and $CuGaSe_2$. Their bandgap energies used in our simulation are 1.035 and 1.68eV.

- Based on Vegard's law, the CIGS lattice parameter is given by the following formula:

$$a_{CIGS}(x) = xa_{CIS} + (1 - x)a_{CGS} \tag{6}$$

For our simulation, the values used for the lattice parameter of $CuInSe_2$ and $CuGaSe_2$ are 5.733and 5.542 Å [26], respectively.

- The deformation induced between $CuIn_{1-x}Ga_xSe_2$ and Si is represented as [26]:

$$\varepsilon_{CIGS/Si} = \frac{a_{Si} - a_{CuIn_{1-x}Ga_xSe_2}}{a_{CuIn_{1-x}Ga_xSe_2}} \tag{7}$$

With a_{Si} and $a_{CuInGaSe2}$ are the lattice constants of silicon and copper indium gallium selenide.

- The absorption coefficient of the direct-band materials used in the simulated structure is given by Ref. [27]:

$$\alpha(\lambda) = \frac{4\pi K(\lambda)}{\lambda} \tag{8}$$

$$\alpha_{CIGS}(x) = x\alpha_{CIS} + (1 - x)\alpha_{CGS} \tag{9}$$

In which K is the extinction coefficient [28], and λ is the wavelength.

Table 1
Basic parameters used in the simulation of the ultra-thin CIGS solar cell.

Contact properties	Front	Back
Surface recombination properties S_e (cm/s)	10^7	10^7
Surface recombination properties S_h (cm/s)	10^7	10^7
Reflectivity R	0.10	0.20

Table 2
Basic parameters used in the simulation of the ultra-thin CIGS solar cell.

Properties of the different layers	Si	CIGS	ZnS	ZnO: Al
Layer thickness d (μm)	1	0.25–2	0,01	0,05
E_g (eV)	1,20	1.07–1.23	3	3.40
Affinity χ(eV)	4,05	4,50	4,15	4,50
Relative permittivity ε_r	11,90	13,60	9	9
Effective density of states N_C(cm^{-3})	$2{,}8.10^{19}$	$2{,}2.10^{18}$	$2{,}2.\ 10^{18}$	$2.2.\ 10^{18}$
Effective density of statesN_V(cm^{-3})	$2{,}65.\ 10^{19}$	$1{,}5.10^{19}$	$1{,}8.\ 10^{18}$	$1{,}8.\ 10^{18}$
Electron mobility μ_n (cm^2/V_s)	1450	100	100	100
Hole mobility μ_p (cm^2/V_s)	500	12.25	25	25
Acceptor or Donor shallow uniform density (cm^{-3})	$1.\ 10^{20}$ (A)	$1.\ 10^{16}$ (A)	$1.\ 10^{18}$ (D)	$1.\ 10^{20}$ (D)
Acceptor or Donor defect density Nt (cm^{-3})	10^{14}(D)	10^{14}(D)	10^{17}(A)	10^{17}(A)

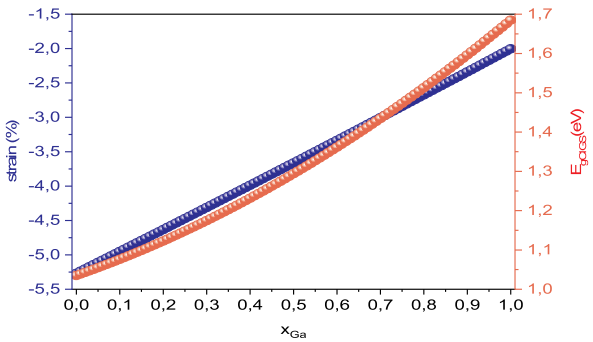

Fig. 3. Strain and band gap energy curves as function of gallium concentration of $CuIn_{1-x}Ga_xSe_2$/Si structure.

- The reflection coefficient R is calculated by the following equation:

$$R(\lambda) = \left(\frac{n_{CIGS} - 1}{n_{CIGS} + 1}\right)^2 \tag{10}$$

Where n_{CIGS} is the refraction index of CIGS [28] and it's given as a function of λ by Vegard's law.

- The external quantum efficiency EQE, is expressed as [29]:

$$EQE(\lambda) = (1 - R(\lambda)).\exp(-\alpha(\lambda).x_i) \tag{11}$$

Tables 1 and 2 illustrate the basic parameters of the different solar cell layers used in our simulation.

3. Results and discussion

In this study, all simulations have been done underneath a sunlight spectrum AM.1.5 provided with an incident power density of 100 mW/cm^2 at room temperature of 300 K. Before starting the simulation of our structure, we focused on the investigation of the most important layer properties (CIGS), such as the band gap energy, the absorption coefficient, the reflection coefficient and the strain of the CIGS/Si system, because these parameters have influenced the solar cell performance. Then, we have studied the gallium concentration as well as the CIGS absorber thickness effects to identify the optimal value of d_{CIGS} and x_{CIGS} taking into account the conversion efficiency. Finally, we have devoted a comparative study to validate our results with experimental data using the same conditions.

The bandgap energy is considered as an important factor in the photovoltaic application. Theoretical conversion efficiency reached its maximum for $E_g = 1.4$–1.5 eV corresponding to x_{Ga} (0.65 and 0.8) in CIGS solar cells [30]. However, experiment revealed that the best efficiency was achieved with $x_{Ga} = 0.2$ to 0.35 [31,32]. According to Fig. 3, we have an increase in the bandgap energy as the

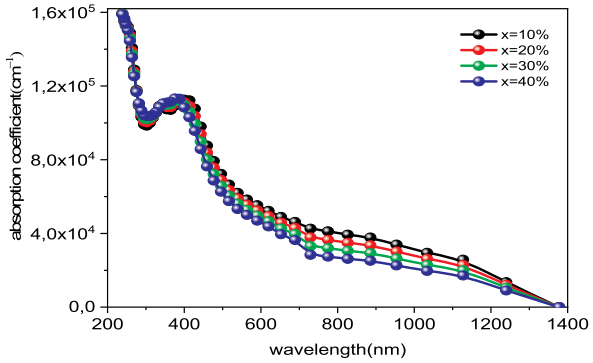

Fig. 4. Absorption coefficient of $CuIn_{1-x}Ga_xSe_2$ for different of gallium concentration.

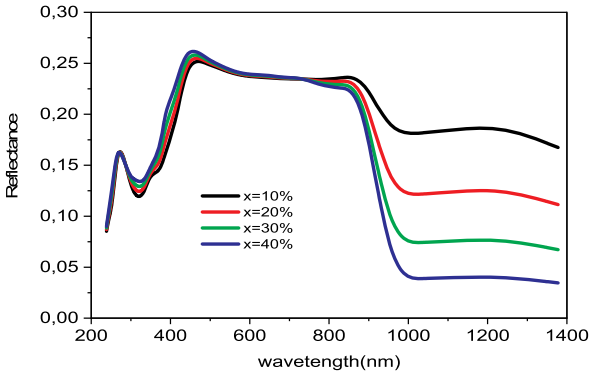

Fig. 5. Reflection coefficient of CIGS as function of λ for different gallium concentration.

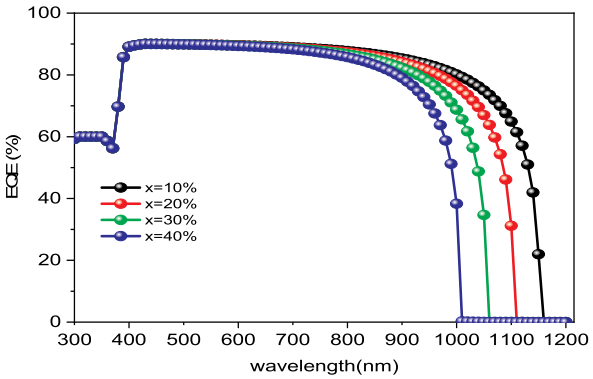

Fig. 6. External quantum efficiency of the CIGS solar cell as function of the wavelength for different gallium concentration.

gallium content increases. The strain in CIGS/Si structure is also presented in Fig. 3. The negative values demonstrate its compressive nature owing to the difference in the lattice parameters of a_{CIGS} and a_{Si}. The strain is in the range of 1.5%–5.5%, and it increases with increasing the Ga content. This proves that CIGS should be grown on Si with low gallium ratio. The best values of energy are assumed to be in the range of 1.13–1.23 eV for $x_{Ga} = 0.2$ to 0.4 in which a low strain appears. In practice, adding Ge, GeSn, GeSi, as a strain reducing layer could be a good solution to minimize the lattice mismatching induced at the interface between CIGS and Si layers [33, 34].

Certainly, the variation of the gallium content affects the optical properties such as the absorption and the reflection coefficients. Fig. 4 depicts the absorption curves of the $CuIn_{1-x}Ga_xSe_2$ alloy for various values of the gallium concentration. We have clearly noted that the absorption curves have the same shape, shift very slightly from each other, and decreases when the wavelength increases. In addition, we notice that when the x_{Ga} increases for wavelength ranges (600–1200 nm) the absorption coefficient decreases. For example, when the gallium concentration increases from 10 to 40% the absorption coefficient becomes $3.10^4 cm^{-1}$, which means that

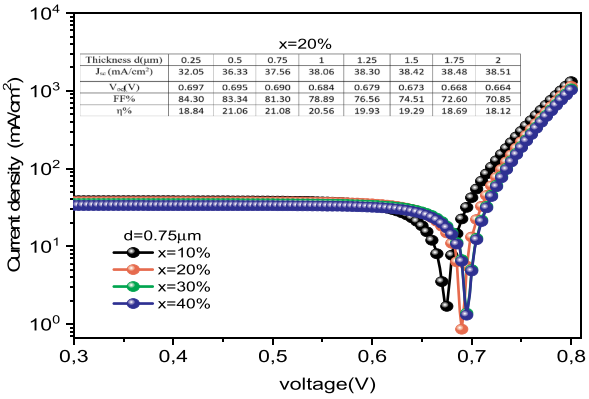

Fig. 7. Variation of the current density I–V according to the voltage V for different gallium concentration.

Table 3
Electrical parameters of $CuIn_{1-x}Ga_xSe_2$/Si for different gallium concentration: J_{sc}, V_{oc}, FF and efficiency.

Gallium concentration (%)	10	20	30	40
J_{sc} (mA/cm^2)	38.61	37.57	37.56	33.46
V_{oc}(V)	0.6731	0.6903	0.6958	0.6958
FF%	79.80	81.30	81.80	81.90
η%	20.74	21.08	20.17	19.07

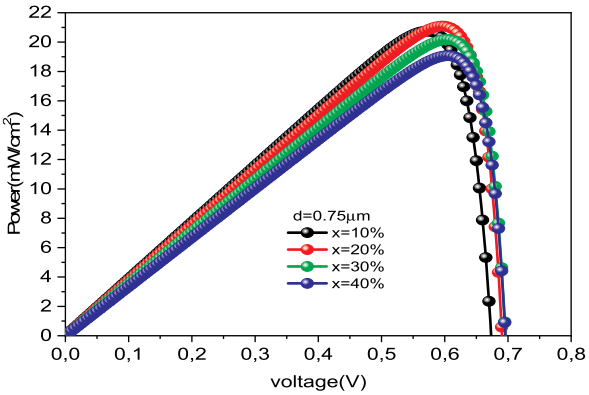

Fig. 8. Power voltage P–V characteristics for different gallium concentration.

we have a relative decrease equal to $\Delta\alpha = 28\%$.

Fig. 5 shows the variation of the reflection coefficient R as a function of wavelengths for various values of x_{Ga}. From the graph, we have revealed that the effect of gallium concentration is clearly observed in higher wavelengths. Mainly, the reflection coefficient is greater for low gallium concentration. This implies higher gallium content in the purpose of reducing the number of reflected photons. In our simulation, we have fixed the reflectivity value at 0.1.

In the range of 400–900 nm, we have reported a low absorption. In contrast, a high reflection occurs. In this case, a lower amount of light enters resulting a lower absorption within the absorber layer [35].

Fig. 6 represents the external quantum efficiency (EQE) data at different gallium concentrations for a fixed value of CIGS thickness (0.75 μm). Varying the gallium concentration from 0.1 to 0.4, the long-wavelength cut-off shifts to the lower values. This shift refers to the decrease in absorption coefficient as x_{Ga} increases according to equation (11). In addition, it is established that for our structure, the x_{Ga} has an impact on the high-wavelength area (low-energy photons are absorbed).

Fig. 7 describes the current density-voltage characteristics J-V at different gallium concentrations. In the range of 0.1–0.4, J_{sc} decreases from 38.61 to 33.46 mA/cm^2.This trend is explained by the reduced number of absorbed photons or even by the important recombination of photogenerated carriers as mentioned in Ref. [36]. However, V_{oc} passes from 0.67 to 0.69 V, improving the fill factor by 2% as shown in Table 3. Indeed, V_{oc} is more important as the collection probability of photocarriers is important. In other words, the rise of the bandgap energy with gallium concentration, reported in Fig. 3, leads to an electric field enhancement, which is responsible for the separation of electron-hole pairs, hence the holes collection at the level of Mo back contact [37].

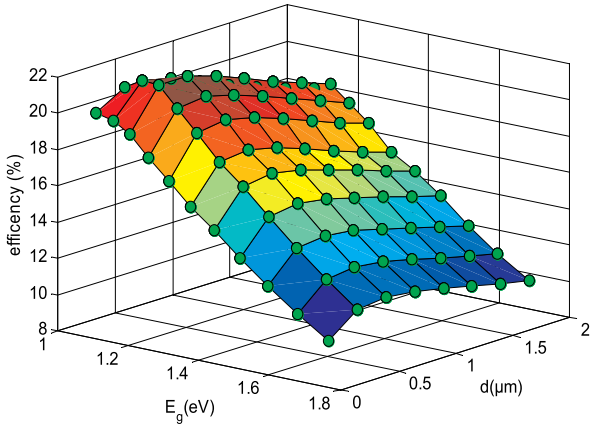

Fig. 9. Conversion efficiency as function of the thickness d and the band gap energy E_g.

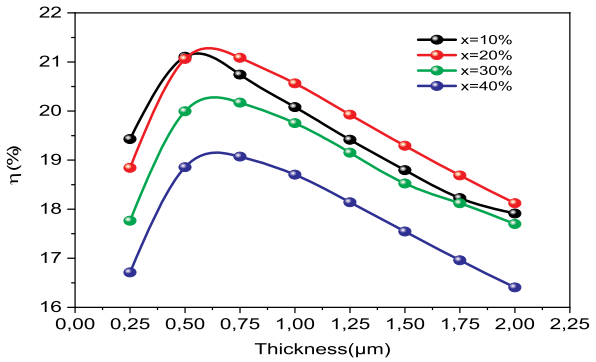

Fig. 10. Conversion efficiency as function of the thickness d for different of gallium concentration.

The power-voltage P–V characteristics as function of gallium concentration are shown in Fig. 8 with maximal power value set at 18–21.5mW/cm^{2}for $d_{CIGS} = 0.75$ μm. We have mentioned that the highest P_{max} is obtained when $x_{Ga} = 0.20$.

The absorber layer thickness is one of the important key parameters that affected the CIGS-based solar cell performance. For this reason, we have plotted in Fig. 9 the conversion yield η as function of CIGS thickness and band gap energy. Varying d_{CIGS} from 0.25 to 0.75 μm have increased the η from 18.81 to 21.08%. Whether d_{CIGS} exceeded 0.75 μm, η decreases considerably from 21.08% to 18.18%. Otherwise, for this critical point d = 0.75 μm, the band gap energy increases from 1 to 1.13 eV achieving an efficiency in the range 19.91–21.08%. However, it decreases dramatically from 21.08 to 11.14% in the range of 1.13–1.68 eV.

Fig. 10 affirms that the thickness and the gallium concentration of CIGS absorber have significantly influenced the performance of our cell. In addition, we have found that the highest conversion efficiency η = 21.08% is reached for optimal values of $d_{CIGS} = 0.75$ μm and $x_{Ga} = 0.20$.

Similarly, to Rajan's work [38], we have taken into consideration the same conditions of series resistance and bulk trap density. Fig. 11(a, b, c, d) shows the effect of CIGS thickness on the photovoltaic parameters (V_{oc}, J_{sc}, FF, η) where we have presented our work accompanied with Rajan's results.

Ranging d_{CIGS} from 0.25 to 0.75 μm, our results have comparatively been in coincidence with simulated and measured parameters in Ref. [38], whereas for $d_{CIGS} > 0.75$ μm, a disagreement has been mentioned. This divergence could refer to the silicon layer. Thus, we have remarkably observed an improvement in all solar parameters for thickness values higher than 0.75 μm. In fact, the decrease of the bulk trap density from 10^{15} to 10^{11} Ref. [38] justified the enhanced values of J_{sc}, V_{oc} and FF. Nevertheless, independently of CIGS thickness, J_{sc} is higher than the measured one. We explained that by the lack of recombination losses at the interface between the silicon layer and the back contact [39].

This study assessed the influence of the bulk defect density combined with the series resistance R_S. Indeed, it has revealed an enhancement in conversion yield up to 21.40%shifting the optimal CIGS thickness from 0.75 to 1 μm (Fig. 11 (d)).

4. Conclusion

To the best of our knowledge, the presented work has investigated numerically a new structure ZnO/ZnS/CIGS/Si/Mo for photovoltaic application employing SCAPS program. We have studied the effects of Ga content and CIGS thickness on opto-electrical of

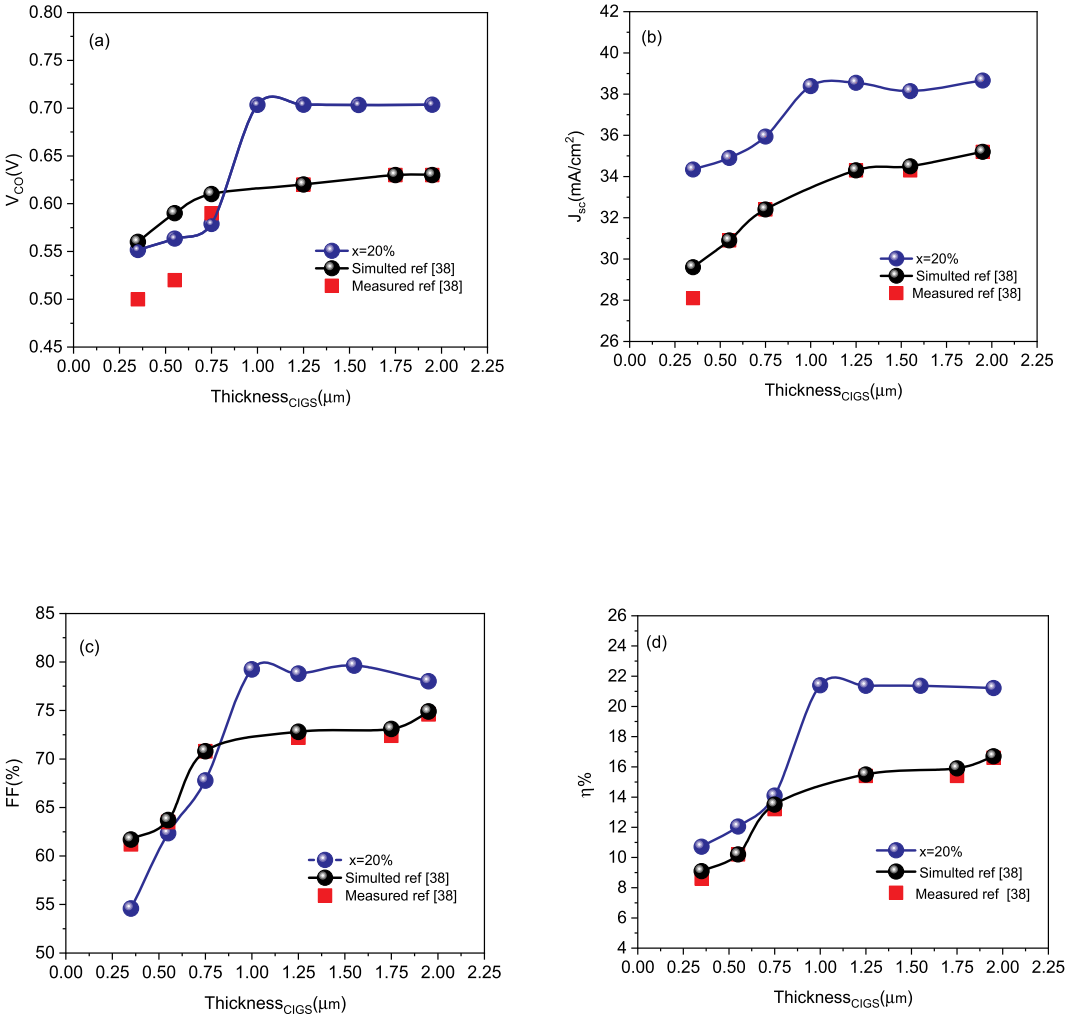

Fig. 11. Evolution of different parameters (a) open-circuit voltage V_{oc}, (b) short-circuit current density J_{sc}, (c) fill factor FF and (d) the conversion efficiency as function of absorber thickness. We validated our results with the simulation and experimental referencing to Ref. [38].

CIGS-based solar cell. The optimal values were $x_{Ga} = 0.20$ and $d_{CIGS} = 0.75$ μm achieving high-efficient yield $\eta = 21.08\%$ under AM.1.5 spectrum. Furthermore, applying the same conditions as the experiments indicates the importance of the bulk defect density and the series resistance on the performance of our structure. Finally, we propose that future work should concentrate on grading ultra-thin CIGS solar cell thanks to its benefits.

References

[1] S. Essig, S. Ward, M.A. Steiner, D.J. Friedman, J.F. Geisz, P. Stradins, D.L. Young, Progress towards a 30% efficient GaInP/Si tandem solar cell, Energy Procedia 77 (2015) 464–469.
[2] S. Essig, M.A. Steiner, C. Allebé, J.F. Geisz, B. Paviet-Salomon, S. Ward, A. Faes, Realization of GaInP/Si dual-junction solar cells with 29.8% 1-sun efficiency, IEEE Journal of Photovoltaics 6 (4) (2016) 1012–1019.
[3] V.M. Lantratov, N.A. Kalyuzhnyĭ, S.A. Mintairov, N. Kh Timoshina, M.Z. Shvarts, V.M. Andreev, High-efficiency dual-junction GaInP/GaAs tandem solar cells obtained by the method of MOCVD, Semiconductors 41 (6) (2007) 727–731.
[4] A. Aissat Nacer, Simulation and optimization of current and lattice matching double-junction GaNAsP/Si solarcells, Superlattice Microstruct. 89 (2016) 242–251S.
[5] M.S. Leite, R.L. Woo, J.N. Munday, W.D. Hong, S. Mesropian, D.C. Law, H.A. Atwater, Towards an optimized all lattice-matched InAlAs/InGaAsP/InGaAs multijunction solar cell with efficiency> 50%, Appl. Phys. Lett. 102 (3) (2013), 033901.
[6] R. Bestam, A. Aissat, J.P. Vilcot, High efficiency quadruple junction solar cells, Superlattice Microstruct. 91 (2016) 22–30.
[7] J.M. Burst, J.N. Duenow, D.S. Albin, E. Colegrove, M.O. Reese, J.A. Aguiar, S. Swain, CdTe solar cells with open-circuit voltage breaking the 1 V barrier, Nature Energy 1 (3) (2016) 16015.
[8] A. Aissat, H. Arbouz, J.P. Vilcot, Optimization and improvement of a front graded bandgap CuInGaSe2 solar cell, Sol. Energy Mater. Sol. Cells 180 (2018) 381–385.
[9] D. Lincot, J.F. Guillemoles, S. Taunier, D. Guimard, J. Sicx-Kurdi, A. Chaumont, O. Roussel, Chalcopyrite thin film solar cells by electrodeposition, Sol. Energy 77 (6) (2004) 725–737.

[10] T.M. Friedlmeier, P. Jackson, A. Bauer, D. Hariskos, O. Kiowski, R. Wuerz, M. Powalla, Improved photocurrent in Cu(In, Ga)Se2 solar cells: from 20.8% to 21.7% efficiency with CdS buffer and 21.0% Cd-free, IEEE Journal of Photovoltaics 5 (5) (2015) 1487–1491.
[11] P. Jackson, R. Wuerz, D. Hariskos, E. Lotter, W. Witte, M. Powalla, Effects of heavy alkali elements in Cu(In, Ga)Se_2 solar cells with efficiencies up to 22.6%, Phys. Status Solidi Rapid Res. Lett. 10 (8) (2016) 583–586.
[12] T.P. White, N.N. Lal, K.R. Catchpole, Tandem solar cells based on high-efficiency c-Si bottom cells: top cell requirements for> 30% efficiency, IEEE Journal of Photovoltaics 4 (1) (2013) 208–214.
[13] M.A. Contreras, M.J. Romero, R. Noufi, Characterization of Cu(In, Ga)Se_2 materials used in record performance solar cells, Thin Solid Films 511 (2006) 51–54.
[14] G. Hanna, A. Jasenek, U. Rau, H.W. Schock, Influence of the Ga-content on the bulk defect densities of Cu(In, Ga)Se_2, Thin Solid Films 387 (1–2) (2001) 71–73.
[15] B. Vermang, J.T. Wätjen, V. Fjällström, F. Rostvall, M. Edoff, R. Gunnarsson, D. Flandre, Highly reflective rear surface passivation design for ultra-thin Cu(In, Ga)Se_2 solar cells, Thin Solid Films 582 (2015) 300–303.
[16] B. Vermang, Bart, J.T. Wätjen, V. Fjällström, F. Rostvall, M. Edoff, R. Kotipalli, D. Flandre, Employing Si solar cell technology to increase efficiency of ultra-thin Cu(In, Ga)Se_2 solar cells, Prog. Photovolt. Res. Appl. 22 (10) (2014) 1023–1029.
[17] M. Gloeckler, Markus, J.R. Sites, Potential of submicrometer thickness Cu(In, Ga)Se_2 solar cells, J. Appl. Phys. 98 (10) (2005) 103703.
[18] L.M. Mansfield, M. Lorelle, A. Kanevce, S.P. Harvey, K. Bowers, C. Beall, S. Glynn, I.L. Repins, Efficiency increased to 15.2% for ultra-thin Cu(In, Ga)Se_2 solar cells, Prog. Photovolt. Res. Appl. 26 (11) (2018) 949–954.
[19] H. Heriche, Z. Rouabah, N. Bouarissa, New ultra-thin CIGS structure solar cells using SCAPS simulation program, Int. J. Hydrogen Energy 42 (15) (2017) 9524–9532.
[20] J. Goffard, C. Colin, F. Mollica, A. Cattoni, C. Sauvan, P. Lalanne, S. Collin, Light trapping in ultrathin CIGS solar cells with nanostructured back mirrors, IEEE Journal of Photovoltaics 7 (5) (2017) 1433–1441.
[21] S. Degrave, M. Burgelman, P. Nollet, Modelling of polycrystalline thin film solar cells: new features in scaps version 2.3, in: Third World Conference on Photovoltaic Energy Conversion IEEE, 2003, pp. 487–490.
[22] Y.J. Hsiao, T.J. Hsueh, J.M. Shieh, M.Y. Yeh, C.C. Wang, B.T. Dai, C. Hu, Bifacial CIGS (11% efficiency)/Si solar cells by Cd-free and sodium-free green process integrated with CIGS TFTs, in: International Electron Devices Meeting IEEE, 2011, pp. 864–867, https://doi.org/10.1109/IEDM.2011.6131686.
[23] H. Movla, Optimization of the CIGS based thin film solar cells: numerical simulation and analysis, Optik 125 (1) (2014) 67–70.
[24] D. Oubda, M.B. Kebre, F. Zougmoré, D. Njomo, F. Ouattara, Numerical simulation of Cu(In, Ga)Se_2 solar cells performances, J. Energy Power Eng. 9 (2015) 1047–1055.
[25] P.D. Paulson, R.W. Birkmire, W.N. Shafarman, Optical characterization of $CuIn_{1-x}Ga_xSe_2$ alloy thin films by spectroscopic ellipsometry, J. Appl. Phys. 94 (2) (2003) 879–888.
[26] T. Fu-Ling, L. Ran, X. Hong-Tao, L. Wen-Jiang, F. Yu-Dong, R. Zhi-Yuan, H. Min, Lattice structures and electronic properties of CIGS/CdS interface: first-principles calculations, Chin. Phys. B 23 (7) (2014), 077301.
[27] J. Geist, A.R. Schaefer, J.F. Song, Y.H. Wang, E.F. Zalewski, An accurate value for the absorption coefficient of silicon at 633 nm, J. res. Natl. Inst. Standards and Technol. 95 (5) (1990) 549.
[28] M.I. Alonso, K. Wakita, J. Pascual, M. Garriga, N. Yamamoto, Optical functions and electronic structure of $CuInSe_2$, $CuGaSe_2$, $CuInS_2$, and $CuGaS_2$, Phys. Rev. B 63 (7) (2001), 075203.
[29] F. Benyettou, A. Aissat, M. Djebari, J.P. Vilcot, Electrical properties of InAsP/Si quantum dot solar cell, Int. J. Hydrogen Energy 42 (30) (2017) 19512–19517.
[30] A. Benmir, M.S. Aida, Analytical modeling and simulation of CIGS solar cells, Energy Procedia 36 (2013) 618–627.
[31] S. Jung, S. Ahn, J.H. Yun, J. Gwak, D. Kim, K. Yoon, Effects of Ga contents on properties of CIGS thin films and solar cells fabricated by co-evaporation technique, Curr. Appl. Phys. 10 (4) (2010) 990–996.
[32] M.A. Contreras, L.M. Mansfield, B. Egaas, J. Li, M. Romero, R. Noufi, W. Mannstadt, Wide band gap Cu (In, Ga) Se_2 solar cells with improved energy conversion efficiency, Prog. Photovolt. Res. Appl. 20 (7) (2012) 843–850.
[33] H. von Känel, F. Isa, C.V. Falub, E.J. Barthazy, E.M. Gubler, D. Chrastina, R. Kaufmann, Three-dimensional epitaxial Si1-XGex, Ge and SiC crystals on deeply patterned Si substrates, ECS Trans. 64 (6) (2014) 631–648.
[34] A. G. Taboada, M. Meduña, M. Salvalaglio, F. Isa, T. Kreiliger, C. V. Falub, E. B. Meier, E. Müller, L. Miglio, G. Isella, H. von Känel. GaAs/Ge crystals grown on Si substrates patterned down to the micron scale. J. Appl. Phys., 119(5), 055301.
[35] M. Xu, A.J. Wachters, J. van Deelen, M.C. Mourad, P.J. Buskens, A study on the optics of copper indium gallium (di) selenide (CIGS) solar cells with ultra-thin absorber layers, Opt. Express 22 (102) (2014) A425–A437.
[36] Y.Y. Jseng, C.J. Chao, H.H. Sung, T.C. Chen, CIGS thin film and device performance produced through a variation Ga concentration during three-stage growth process, Mater. Sci. Semicond. Process. 87 (2018) 162–166.
[37] M. Saadat, M. Moradi, M. Zahedifar, CIGS absorber layer with double grading Ga profile for highly efficient solar cells, Superlattice Microstruct. 92 (2016) 303–307.
[38] G. Rajan, K. Aryal, S. Karki, P. Arya, R.W. Collins, S. Marsillac, Characterization and analysis of ultrathin CIGS films and solar cells deposited by 3-stage process, J. Spectrosc. ume (2018) 9.
[39] Z. Jehl, F. Erfurth, N. Naghavi, L. Lombez, I. Gerard, M. Bouttemy, W. Wischmann, Thinning of CIGS solar cells: part II: cell characterizations, Thin Solid Films 519 (21) (2011) 7212–7215.